

MmWave Beam Prediction with Situational Awareness: A Machine Learning Approach

(Invited Paper)

Yuyang Wang[‡], Murali Narasimha[§] and Robert W. Heath Jr.[‡]

[‡] Department of Electrical and Computer Engineering, The University of Texas at Austin, USA

[§] Huawei Technologies, USA

Email: {yuywang, rheath}@utexas.edu, murali.narasimha@huawei.com

Abstract—Millimeter-wave communication is a challenge in the highly mobile vehicular context. Traditional beam training is inadequate in satisfying low overheads and latency. In this paper, we propose to combine machine learning tools and *situational awareness* to learn the beam information (power, optimal beam index, etc) from past observations. We consider forms of situational awareness that are specific to the vehicular setting including the locations of the receiver and the surrounding vehicles. We leverage regression models to predict the received power with different beam power quantizations. The result shows that situational awareness can largely improve the prediction accuracy and the model can achieve throughput with little performance loss with almost zero overhead.

I. INTRODUCTION

Configuring millimeter wave (mmWave) antenna arrays is a challenging task in vehicular applications [1], [2]. With high mobility, vehicles suffer from intermittent blockages from trucks, buses, etc, and therefore potential coverage holes, which requires frequent beam re-alignment to maintain transmission links with high data rates [3]. Current solutions adopted in IEEE 802.11ad is inadequate in satisfying the low overheads and latency requirement in many vehicular applications [4], [5]. MmWave, though, is the only viable solution to support massive data sharing and is incredibly valuable for infotainment services, with the emerging applications in 5G vehicular/cellular communication [6–8]. Consequently, low overhead methods with high efficiency and robustness need to be designed to enable fast configuration of millimeter wave links.

One alternative to simplify beamforming in mmWave vehicular networks is to make use of out-of-band side information [9]. *Side information* is ubiquitous in intelligent transportation systems. Vehicles have a number of sensors including GPS, radar, LIDAR, and cameras. In addition, connectivity between vehicles allows exchange of such information, which equips the vehicles with *situational awareness* [10], [11]. In [9], [12], out-of-band information assisted mmWave beam training was proposed to leverage the data from sensors or other communication systems. In [13], it was argued that there exists congruency between the channel at mmWave and sub-6 GHz bands, which can be leveraged to do beam selection and channel estimation. In [14], a beam alignment solution was designed by extracting useful information from radar signal to configure the antennas and design beams at vehicles.

An inverse fingerprinting approach was proposed to facilitate optimal beam pair selection in [1]. Given the receiver location, the infrastructure recommends and ranks the beams based on the occurrences of optimal beam pair in the dataset for that location. In [15], a framework of generating 5G MIMO dataset using ray tracing was proposed, and deep learning model was applied to assist in mmWave beam selection with temporally-correlated vehicle moving trajectories.

In this paper, we propose a novel framework to leverage machine learning tools with the availability of *situational awareness*, in predicting mmWave beam power. In the vehicular contexts, road side buildings and infrastructures are stationary, and pedestrians are small in size, which makes vehicles the most important mobile reflectors in the urban canyons. The situational awareness of the vehicles, therefore, can be mapped to the received power of different beams. We propose to use the vehicle locations as features to predict the received power of *any beam* in the beam codebook, with low or almost-zero feedback overhead. Vehicle locations may be obtained from the basic safety message in dedicated short-range communications (DSRC), or through similar functionality in a cellular system. First, we apply different regression models over the *strongest beam power* [16]. We compare the results with different levels of situational awareness and show that full situational awareness can largely improve the prediction accuracy. We also investigate how different channel quality indicator (CQI) quantization parameters can effect the results using our specific dataset. We show that the optimal parameters depend on the dataset statistics and CQI quantization does not degrade the performance much, if high resolution can be guaranteed. Lastly, we evaluate the performance of multivariate regression over power of all beam pairs. We observe that beam selection based on the power prediction can achieve higher throughput compared to that based on classification.

II. DATABASE ESTABLISHMENT

A. Simulation setup

In this paper, we set the analysis in a two-lane straight street in the urban canyon, as shown in Fig. 1. Building placements are predetermined. The road-side unit (RSU) is deployed at the road side, at the height of 5 meters, and there are two types of vehicles in the environments, respectively the trucks (with identical sizes of length, height, width = T_ℓ, T_h, T_w) and low

height cars with size of C_ℓ, C_h, C_w . We use *Wireless Insite* from *Remcom* to obtain the channel and beam information [17]. We only simulate the channels of low-height cars since high trucks are free of blockage, and the optimal beam pair is always line-of-sight (LOS).

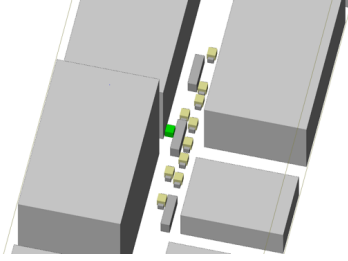


Fig. 1. An illustration of the urban canyon in the ray tracing simulation. Fixed buildings are deployed at the roadside. The green box represents the RSU, and the receivers (yellow boxes) are mounted on top of the low-height cars. Vehicles are randomly dropped on the two lanes, under some certain vehicle density and truck-to-car ratio.

B. Channel model

We generate the mmWave channel by combining the outputs from ray tracing and the geometric channel model [1]. The *rays* in ray tracing are equivalent to the *paths* in mmWave channel modeling. From the ray tracing output, we obtain the path information $\{\phi_\ell^A, \theta_\ell^A, \phi_\ell^D, \theta_\ell^D, \tau_\ell, a_\ell\}$, $\ell \in \{1, 2, \dots, L\}$ of the strongest L rays, where $(\phi_\ell^A, \theta_\ell^A)$ are the azimuth and elevation angles of arrival, while $(\phi_\ell^D, \theta_\ell^D)$ are the azimuth and elevation angles of departure. And a_ℓ is the path gain for the ℓ -th ray, and τ_ℓ is the time of arrival. We deploy 4×2 ($N_t = N_r = 8$) uniform planar arrays at both the transmitter and receiver sides. We define $g(\cdot)$ as the pulse shaping filter, and approximate the channel matrix $\mathbf{H}[n]$, $n = 0, 1, \dots, L_c - 1$ by the geometric channel model

$$\mathbf{H}[n] = \sqrt{N_t N_r} \sum_{\ell=1}^L g(nT - \tau_\ell) \mathbf{a}_r(\phi_\ell^A, \theta_\ell^A) \mathbf{a}_t^*(\phi_\ell^D, \theta_\ell^D) a_\ell, \quad (1)$$

where T is the symbol period, $\mathbf{a}_r(\phi_\ell^A, \theta_\ell^A)$ and $\mathbf{a}_t^*(\phi_\ell^D, \theta_\ell^D)$ are the steering vectors at the arrival and departure sides for uniform planar arrays. We apply DFT codebook for the precoder and combiner [18]. Therefore, there are in total of $N_B = N_t N_r = 64$ different beam pairs in our dataset. Assume the i -th beam pair, $(\mathbf{w}_i, \mathbf{f}_i)$, $i \in \{1, 2, \dots, N_B\}$, is selected from the codebook, the received power y_i can be calculated as

$$y_i = \sum_{n=0}^{L_c-1} |\mathbf{w}_i^* \mathbf{H}[n] \mathbf{f}_i|^2. \quad (2)$$

The training label for beam power regression is $\mathbf{y} = [y_1, y_2, \dots, y_{N_B}]$, and the corresponding optimal beam pair can be derived by $s = \operatorname{argmax}_{i \in \{1, \dots, N_B\}} y_i$.

C. Power quantization

In mmWave systems, after beam sweeping is implemented, the infrastructure cannot obtain the *exact* value of received

TABLE I
AN EXAMPLE OF THE DATASET AND THE POST-PROCESSING

Original	$\ell_i = y_1, \dots, y_{N_B}$
CQI	$\ell_c = \mathcal{Q}(y_1), \dots, \mathcal{Q}(y_{N_B})$
Regressor	$\ell_r = r(\mathcal{Q}(y_1)), \dots, r(\mathcal{Q}(y_{N_B}))$
Ordered beam	$\ell_m(N) = r(\mathcal{Q}(\bar{y}_1)), \dots, r(\mathcal{Q}(\bar{y}_M))$

power by channel feedback. Generally, only the quantized CQIs along with the corresponding beam pair indexes are fed back to the infrastructure. Hence, the continuous received power from simulation, which is obtained from (2), in *first* row of Table I and represented by ℓ_i , needs to be quantized by some certain quantization rule. There is a vast body of literature discussing different mapping schemes from received power to CQI [19], [20]. In Long Term Evolution (LTE), CQI is an indication of what modulation and coding scheme (MCS)/transport block the UE can reliably receive. Specifically, the UE determines the highest MCS for which the block error rate is under 10%, in the bandwidth in which the CSI reference signal is received. Our case is different from the CQI calculation in LTE, since we are not primarily concerned about the appropriate selection of MCS at this point. Instead, we target at predicting the beam power, and transmitting the precise information of the received power to the infrastructure for regression. Therefore, in our case, CQI is a direct indicator of reference signal received power (RSRP). For simplicity, we assume a simple *uniform quantization scheme*, where we use P_u and P_ℓ to *upper* and *lower bound* the power. We then define the CQI *granularity* as r_{CQI} , and the relationship between the received power p and the CQI index q is defined by

$$\mathcal{Q}(p) = \left\lceil \min \left\{ \max \left\{ \frac{p - P_\ell}{r_{\text{CQI}}}, 0 \right\}, \frac{P_u - P_\ell}{r_{\text{CQI}}} \right\} \right\rceil, \quad (3)$$

where the idea is to upper bound the received power by P_u (CQI = $\mathcal{Q}(P_u)$) and lower bound it by P_ℓ (CQI = 0), and then quantize evenly for the power lying in the range $p \in [P_\ell, P_u]$. And correspondingly, we recover the continuous received power from the CQI by

$$r(q) = r_{\text{CQI}} q + P_\ell. \quad (4)$$

After CQI quantization, the entropy of the information is reduced, and quantization inaccuracy is introduced, especially for the power out of the range $[P_\ell, P_u]$, which is either *upper* or *lower bounded*. In Section IV, we will show that the learning accuracy depends on the aforementioned parameter P_u , P_ℓ and the quantization granularity. Even with low quantization resolution, however, we show that performance is not degraded significantly.

III. LEARNING MODEL

In this section, we explain the rule of encoding the situational features and the approach to predict the beam power. We show that the power prediction is able to predict *any* beam, e.g., the strongest beam, second strongest beam, etc. It is also

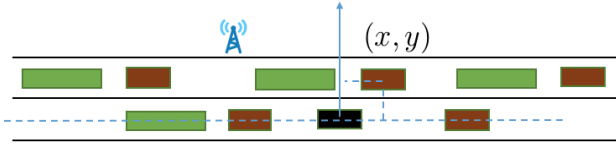


Fig. 2. A demonstration of the vehicle's geometry and encoding. The black car is the receiver. The brown boxes are the small-size cars surrounding the receiver. The green boxes denote the surrounding trucks.

applicable to the predict the beam power based on the beam pair index.

A. Encoding the geometry

There are different ways to encode the vehicles' situational awareness. Since we deploy two types of vehicles (cars and trucks) randomly on a two-lane street, we need to design the appropriate scheme to encode the geometry and order the features accordingly. Specifically, we apply simple *Cartesian coordinate* to encode the locations, as demonstrated in Fig. 2. The origin of the Cartesian coordinate is set as the receiver, and the road-side unit and the surrounding vehicles are encoded accordingly under the current coordinate. Also, we can observe from the vehicle deployments that generally for a receiver, it is easier to be blocked and effected by the vehicle on the first lane, i.e., the lane closer to the RSU. Furthermore, large trucks and vehicles that are closer by have more impact on the receiver's beam. Hence, we propose the following strategy to encode and order the geometry.

The feature \mathbf{v} is a one-dimensional vector and can be generated by

$$\mathbf{v} = [\mathbf{r}, \mathbf{t}_1, \mathbf{t}_2, \mathbf{c}_1, \mathbf{c}_2]. \quad (5)$$

In (5), \mathbf{r} is the location of the RSU in the Cartesian coordinate, \mathbf{t} represents the truck and \mathbf{c} denotes the low-height cars. The subscripts 1 and 2 denote the lane index where the vehicle is located on. For the trucks on the first lane, e.g., given the coordinates of the trucks along the x -axis on the first lane in the Cartesian coordinate as $[x_1, x_2, \dots, x_n]$, \mathbf{t}_1 is composed of the locations of the trucks in the following order.

$$\mathbf{t}_1 = [x_{i_1}, y_{i_1}, x_{i_2}, y_{i_2}, \dots, x_{i_N}, y_{i_N}], \quad (6)$$

$$|x_{i_1}| < |x_{i_2}| < \dots < |x_{i_N}|.$$

Here, we constrain the number of trucks/cars on each lane as the maximum number of N in order to make dimensions of features consistent under different deployment scenarios. If the number of trucks $n > N$, we *delete* the locations of $N - n$ trucks that are located far away from the feature; otherwise, we add in $n - N$ *virtual* trucks that are lying very far away, where $x = \infty$ (we choose $x = 10^4$ here). Similarly, the trucks/cars on the different lanes can be encoded.

B. Practical issues with feedback

In implementations, the feedback link conveys the information of only a subset of the beam pairs. Generally, the feedback

includes the best M beams' received power and the corresponding beam pair index. With limited information of the beam pairs' power, we rearrange the beam pairs in decreasing order of their powers, i.e., $\bar{y}_1 > \bar{y}_2, \dots, > \bar{y}_M \dots, > \bar{y}_{N_B}$, and only apply regressor to the first M beams' received power, as shown in the *fourth* row of Table I. The model eliminates the necessity of feeding back information of all beams and can be combined with other models that can rank the beams correspondingly, to achieve even lower overheads. In this paper, we focus on the analysis of only the beam pair with the *strongest power*, i.e., $M = 1$.

We also consider the case that *unordered* beam power, as shown in the *first* row of Table I, needs to be fed back to the infrastructures. Larger overheads are introduced to the system and a longer time is required to finish the database establishment. The *full knowledge* of the beams' power, however, provides an easy way to select and recommend the optimal beam pair, and also to evaluate the system performance.

IV. PERFORMANCE EVALUATION

In this section, we train the regressors with different learning models and datasets, to predict the power of each beam. We define the relevant performance metrics, and evaluate the system performance with different features and CQI quantization parameters. Then we examine the performance when power is predicted per beam pair.

A. Performance metric definition

Let $\max\{\cdot\}$ denote the maximum element of the vector (\cdot) , and $\arg \max\{\cdot\}$ the index of the maximum value and $\mathbb{1}(\cdot)$ is the indicator function. Given the real power $\mathbf{Y} = \{y_1, \dots, y_m\}$, and the predicted power $\hat{\mathbf{Y}} = \{\hat{y}_1, \dots, \hat{y}_m\}$, the *alignment probability* can be formulated as $P_A = \frac{1}{m} \sum_{i=1}^m \mathbb{1}(\arg \max\{y_i\} = \arg \max\{\hat{y}_i\})$. And we can further define *achieved throughput ratio* R_T as

$$R_T = \frac{\sum_{i=1}^m \log_2(1 + y_i[\arg \max\{\hat{y}_i\}])}{\sum_{i=1}^m \log_2(1 + \max\{y_i\})}. \quad (7)$$

Achieved throughput ratio R_T indicates the system performance in throughput when the system is deployed simply relying on the learning model without beam training.

B. Regression models

Using the situational features defined in Section III-A, we compare results with different regression models. We utilize the root mean squared error (RMSE) to quantify the regression accuracy over the *strongest beam power*, i.e., \bar{y}_1 , in dB scale. Specifically, we compare the prediction results among linear regression, support vector regression, Random Forest regression and gradient boosting regression in Table II. It is shown that the Random Forest is a good fit for our specific dataset, since it is able to implicitly select the features and generalizes well by ensembles. Also, the Random Forest is fast to train and is a promising learning method that could be applicable in industry field implementations.

TABLE II
REGRESSION RMSE OVER THE STRONGEST BEAM POWER USING DIFFERENT REGRESSION ALGORITHMS.

	RMSE (dBm)
Linear regr	6.199
SVR	3.645
Random Forest	1.726
Gradient Boosting	2.814

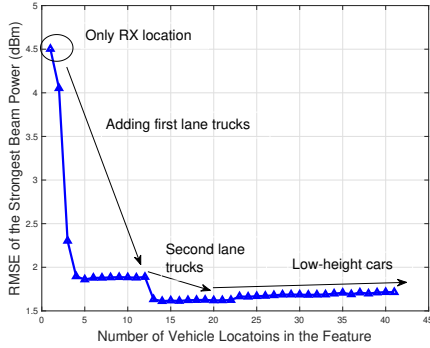


Fig. 3. Comparison of alignment with different levels of situational awareness.

C. Different levels of situational awareness

In this section, we show how situational awareness can help to predict the beam power. Current pathloss model relies on the relative distance [8] or the absolute locations of the receiver and the transmitter [21]. Result in [1] also showed that the receiver location only can provide useful information about the beam by exploiting dataset of previous transmissions. Here we show that in an urban vehicular context, the environment information of vehicle locations could be leveraged for more accurate prediction of the beam power. Based on the vehicle location *order* in Section III-A, in Fig. 3, we plot the RMSE of the strongest beam pair using the Random Forest regressor with the *first* i -th vehicles' locations in the feature as explained in Section III-A. It could be observed that the first lane trucks' locations provide abundant information about the beam power. RMSE is reduced from 4.5 to around 1.7, compared to the case when only the receiver location is used as the feature. More truck locations on the second lane finally reduce the RSME to around 1.6. Low-height cars, however, do not further help beam prediction. Slight degradations of RMSE are shown when extra cars' locations are fed in the feature. Hence, we conclude that the high trucks' locations, especially those on the first lane, are more relevant in predicting the beam power and a concise set of location features are sufficient in providing good predictions.

D. CQI Quantization

In this section, we compare the performance of the strongest beam pair power prediction with CQI quantization. Specifically, we quantize the power first and recover the continuous power as explained in Section II-C. We evaluate the RMSE

TABLE III
ALIGNMENT PROBABILITY AND ACHIEVED THROUGHPUT RATIO WITH DIFFERENT CQI QUANTIZATION GRANULARITIES.

	P_A (%)	R_T (%)
Classifier	84.6	98.4
No QT	82.0	98.8
$r_{CQI} = 1$	81.1	98.8
$r_{CQI} = 2$	79.2	98.7
$r_{CQI} = 5$	72.6	97.8

of prediction using different combinations of parameters r_{CQI} , P_u and P_ℓ . It is observed from the dataset that the highest beam power across the dataset is $P_{\max} = 44.23$ dBm and the lowest power is $P_{\min} = -15.15$ dBm. Based on these, we select the combinations of P_u and P_ℓ as shown in Fig. 4. It is shown that the RMSE increases with a larger granularity generally. In the small quantization granularity regime, e.g., $r_{CQI} = 0, 0.1, 0.2, 0.5, 1$ dBm, there are no significant differences among the RMSEs. Also, the larger upper bound P_u gives more accurate predictions, while the lower bound P_ℓ has negligible impact. The reason is that the power of the strongest beam power is generally large and a *small upper bound* will bring large errors by quantization. It should be noted, however, that both the upper and lower bound needs to be carefully designed in order to guarantee the quantization accuracy with the given statistics of the datasets.

Fig. 5 further compares the cumulative density function (CDF) of the regression error $|y_{\text{pred}} - y_{\text{true}}|$ with different quantization granularities. The three dots in red, blue and black indicate the probabilities that the regression error is smaller than 1 dBm. It is shown that with $r_{CQI} = 1$ or 2 dBm, we can still guarantee error of more than 50% of the predictions to be smaller than 1 dBm. And there is barely any difference between the accuracy using 1 dBm quantization and the case without quantization.

E. Regression over all beam pairs

Previous results apply a regression model over the strongest beam power. In this section, we predict the power based on the beam pair index as defined in (2). The advantage of this method is that it gives extra information to the order of the beam pair power, and helps to select the beam pair for data transmission. This case, however, requires the knowledge of the power of *all* beam pairs, which introduces larger overheads to establish the dataset. Here, we focus on evaluating how the power prediction can be helpful in assisting the beam selection, without considering the overhead issues. We compare the alignment probability P_A and the achieved throughput R_T as defined in Section IV-A, using different quantization granularities of CQI and the case when we simply apply a classifier over the optimal beam pair index. Similarly as Section IV-D, quantization with high resolution does not introduce a lot of performance degradation. Also, even though the alignment probabilities P_A with the regression models are lower than

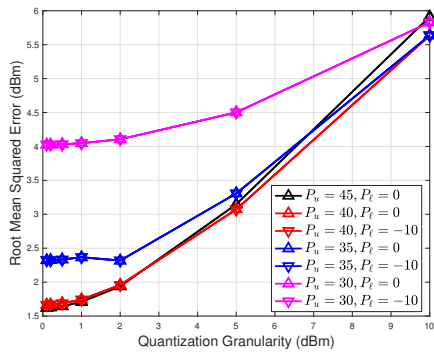


Fig. 4. Comparison of RMSE using different selections of quantization parameters P_u , P_l and r_{CQI} . Specifically, we consider some combinations of $P_u = 45, 40, 35, 30$ dBm, and $P_l = 0, -10$ dBm and quantization granularity $r_{\text{CQI}} = 0.1, 0.2, 0.5, 1, 2, 5, 10$ dBm.

the classifier, the achieved throughputs are higher than that of the classification. More beams' power provides intrinsic information about the beam power orders. Lastly, the achieved throughput ratios are all very high due to the fact that there are not big differences among the power of the top beams. The results show that our model is good at identifying the "good" beams from the "bad" beams, even though 100% alignment probability cannot be achieved.

V. ACKNOWLEDGMENTS

This research was partially supported by a gift from Huawei through UT Situation-Aware Vehicular Engineering Systems (UT-SAVES), and by the U.S. Department of Transportation through the Data-Supported Transportation Operations and Planning (D-STOP) Tier 1 University Transportation Center and Communications and Radar-Supported Transportation Operations and Planning (CAR-STOP) project funded by the Texas Department of Transportation.

REFERENCES

- [1] V. Va, J. Choi, T. Shimizu, G. Bansal, and R. W. Heath, "Inverse multipath fingerprinting for millimeter wave V2I beam alignment," *IEEE Trans. Veh. Technol.*, vol. PP, no. 99, pp. 1–1, 2017.
- [2] J. Wang, "Beam codebook based beamforming protocol for multi-Gbps millimeter-wave WPAN systems," *IEEE J. Sel. Areas Commun.*, vol. 27, no. 8, 2009.
- [3] Y. Wang, K. Venugopal, A. F. Molisch, and R. W. Heath, "Blockage and coverage analysis with mmwave cross street BSs near urban intersections," in *Proc. IEEE Int. Conf. Commun. (ICC)*, pp. 1–6, May 2017.
- [4] S. Sur, V. Venkateswaran, X. Zhang, and P. Ramanathan, "60 GHz indoor networking through flexible beams: A link-level profiling," in *ACM SIGMETRICS Performance Evaluation Review*, vol. 43, pp. 71–84, ACM, 2015.
- [5] T. Nitsche, C. Cordeiro, A. B. Flores, E. W. Knightly, E. Perahia, and J. C. Widmer, "IEEE 802.11 ad: directional 60 GHz communication for multi-Gigabit-per-second Wi-Fi," *IEEE Commun. Mag.*, vol. 52, no. 12, pp. 132–141, 2014.
- [6] J. Choi, V. Va, N. Gonzalez-Prelcic, R. Daniels, C. R. Bhat, and R. W. Heath, "Millimeter-wave vehicular communication to support massive automotive sensing," *IEEE Commun. Mag.*, vol. 54, pp. 160–167, December 2016.

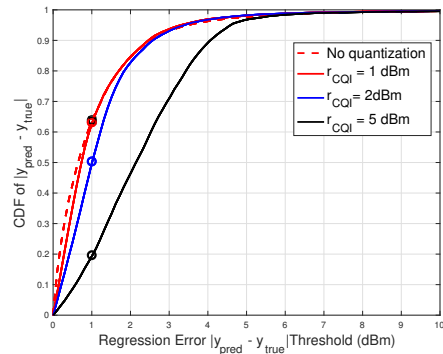


Fig. 5. Comparison of regression error $|y_{\text{pred}} - y_{\text{true}}|$ with different CQI quantization granularities $r_{\text{CQI}} = 1, 2, 5$ dBm and the case without CQI quantization. The y coordinates of the three circles (in red, blue and black) represent the probability that the regression error is smaller than 1 dB.

- [7] T. S. Rappaport, R. W. Heath Jr, R. C. Daniels, and J. N. Murdock, *Millimeter wave wireless communications*. Pearson Education, 2014.
- [8] T. S. Rappaport, S. Sun, R. Mayzus, H. Zhao, Y. Azar, K. Wang, G. N. Wong, J. K. Schulz, M. Samimi, and F. Gutierrez, "Millimeter wave mobile communications for 5G cellular: It will work!," *IEEE Access*, vol. 1, pp. 335–349, 2013.
- [9] N. Gonzalez-Prelcic, A. Ali, V. Va, and R. W. Heath, "Millimeter-wave communication with out-of-band information," *IEEE Commun. Mag.*, vol. 55, pp. 140–146, DECEMBER 2017.
- [10] J. Wei, J. M. Snider, J. Kim, J. M. Dolan, R. Rajkumar, and B. Litkouhi, "Towards a viable autonomous driving research platform," in *Proc. IEEE Intell. Veh. Symp. (IV)*, pp. 763–770, IEEE, 2013.
- [11] R. Rasshofer and K. Gresser, "Automotive radar and LiDAR systems for next generation driver assistance functions," *Advances in Radio Science*, vol. 3, no. B. 4, pp. 205–209, 2005.
- [12] T. Nitsche, A. B. Flores, E. W. Knightly, and J. Widmer, "Steering with eyes closed: mm-wave beam steering without in-band measurement," in *Computer Communications (INFOCOM), 2015 IEEE Conference on*, pp. 2416–2424, IEEE, 2015.
- [13] A. Ali, N. Gonzalez-Prelcic, and R. W. Heath, "Millimeter wave beam-selection using out-of-band spatial information," *IEEE Trans. Wireless Commun.*, vol. 17, pp. 1038–1052, Feb 2018.
- [14] N. Gonzalez-Prelcic, R. Méndez-Rial, and R. W. Heath, "Radar aided beam alignment in mmwave V2I communications supporting antenna diversity," in *Proc. Inf. Theory and Appl. Workshop (ITA)*, pp. 1–7, Jan 2016.
- [15] A. Klautau, P. Batista, N. G. Prelcic, Y. Wang, and R. W. Heath, "5G MIMO data for machine learning: Application to beam-selection using deep learning," in *Proc. Inf. Theory and Appl. Workshop (ITA)*, pp. 1–6, Jan. 2016.
- [16] https://github.com/yuyangwang/spawc_regression_power.
- [17] <https://www.remcom.com/wireless-insite-em-propagation-software/>.
- [18] D. Yang, L.-L. Yang, and L. Hanzo, "DFT-based beamforming weight-vector codebook design for spatially correlated channels in the unitary precoding aided multiuser downlink," in *Proc. IEEE Int. Conf. Commun. (ICC)*, pp. 1–5, IEEE, 2010.
- [19] H. Huawei, "Interference measurement resource configuration and CQI calculation," in *3GPP Draft: R1-121947, TSG RAN WGI Meeting*, vol. 69, pp. 21–25, 2012.
- [20] J. Lee, J.-K. Han, and J. Zhang, "MIMO technologies in 3GPP LTE and LTE-advanced," *EURASIP J. Wireless Commun. and Netw.*, vol. 2009, p. 3, 2009.
- [21] Y. Wang, K. Venugopal, R. W. Heath, and A. F. Molisch, "MmWave vehicle-to-infrastructure communication: Analysis of urban microcellular networks," *IEEE Trans. Veh. Technol.*, 2018.